ACS central science

Research Article

http://pubs.acs.org/journal/acscii

Modulation of Innate Immune Responses *via* Covalently Linked TLR Agonists

Janine K. Tom,[†] Emmanuel Y. Dotsey,[‡] Hollie Y. Wong,[†] Lalisa Stutts,[†] Troy Moore,[†] D. Huw Davies,[‡] Philip L. Felgner,[‡] and Aaron P. Esser-Kahn*[,†]

[†]Department of Chemistry and [‡]Department of Medicine, Division of Infectious Diseases, University of California, Irvine, Irvine, California 92697, United States

Supporting Information

ABSTRACT: We present the synthesis of novel adjuvants for vaccine development using multivalent scaffolds and bioconjugation chemistry to spatially manipulate Toll-like receptor (TLR) agonists. TLRs are primary receptors for activation of the innate immune system during vaccination. Vaccines that contain a combination of small and macromolecule TLR agonists elicit more directed immune responses and prolong responses against foreign pathogens. In addition, immune activation is enhanced upon stimulation of two distinct TLRs. Here, we synthesized combinations of TLR agonists as spatially defined tri- and di-agonists to understand how specific TLR agonist combinations contribute to the overall immune response. We covalently conjugated three TLR agonists (TLR4, 7, and 9) to a small molecule core to probe the spatial arrangement of the agonists. Treating immune cells with the linked agonists increased activation of the transcription factor NF-κB and enhanced and directed immune related cytokine production and gene expression beyond cells treated with an unconjugated mixture of the same three agonists. The use of TLR signaling inhibitors and knockout studies confirmed that the tri-agonist molecule activated multiple signaling pathways leading to the observed higher activity. To validate that the TLR4, 7, and 9 agonist combination would activate the immune response to a greater extent, we performed *in vivo* studies using a vaccinia vaccination model. Mice vaccinated with the linked TLR agonists showed an increase in antibody depth and breadth compared to mice vaccinated with the unconjugated mixture. These studies demonstrate how activation of multiple TLRs through chemically and spatially defined organization assists in guiding immune responses, providing the potential to use chemical tools to design and develop more effective vaccines.

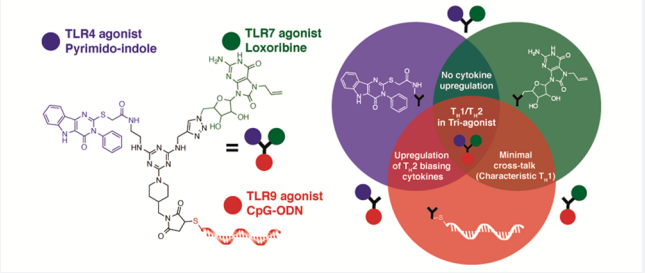

INTRODUCTION

Vaccines are powerful and effective tools for disease prevention, treatment, and even elimination.[1,2] Many effective, whole pathogen vaccines activate the innate immune system through synergistic interactions of multiple immune cell receptors, where Toll-like receptor (TLR) synergies are the most established.[1,3,4] TLR agonists are defined molecular entities, ranging from oligonucleotides to heterocyclic small molecules, which are used as vaccine adjuvants that enhance the immune response against a coadministered antigen.[5−11] However, individual TLR agonists are not as effective as whole pathogens. Many TLR agonists combinations influence immune signaling pathways both spatially and temporally.[12−19] Until recently, understanding how the spatial organization of multiple TLR agonists affects TLR activation and the overall immune response has been difficult, as probing synergies has been limited to combining mixtures of TLR agonists in solution. Therefore, removing the defined spatial arrangement of native agonists in a pathogen.[3,12,15,16,20−23]

To determine how spatial arrangement affects immune synergies and to eliminate diffusion issues, a single molecular entity that activates multiple receptors is needed. Here, we covalently conjugated three TLR agonists *via* a tri-functional, small molecule core and correlated how the specific spatial arrangement directly controlled innate immune cell activation. We observed that treatment with the tri-agonist compound produced a distinct array of cytokines *in vitro*, and this activity translated *in vivo* to generate a wider set of antibodies against a model vaccinia vaccine.

In recent years, the conjugation of up to two TLR agonists has been explored, where treatment with covalently conjugated TLR agonists can generate immune responses that are synergistic or repressive.[24−27] However, the components of many vaccines activate three to five TLRs. A prime example is the Yellow Fever Vaccine, one of the most successful vaccines, which activates four different TLRs (2, 7, 8, and 9).[1,28,29] Some of these enhanced synergies are postulated to result from cooperation between MyD88 and TRIF adaptor proteins that are downstream from TLR activation and modulate changes in transcription.[30−35] As a result, our working hypothesis was that stimulating a specific set of TLRs on one cell *via* covalent

Received: August 5, 2015
Published: October 28, 2015

DOI: 10.1021/acscentsci.5b00274
ACS Cent. Sci. 2015, 1, 439−448

linkage of three TLR agonists would activate a distinct pattern of cell-signaling molecules as measured by transcription. If each molecular combination yields a distinct immune response profile, then the synthetic, spatial manipulation of TLR agonists could guide a particular immune response. To gain a better understanding of TLR synergies, we covalently attached three agonists together allowing spatially defined activation of three distinct TLRs.

Here, we present the conjugation of pyrimido[5,4-*b*]indole, loxoribine, and CpG-ODN1826, TLR4, 7, and 9 agonists, respectively, into a single tri-agonist compound. TLR7 and 9 are endosomal receptors, while TLR4 is located on the cell surface and in the endosome. Once stimulated, each TLR activates a specific immune signaling pathway.[36,37] TLR4, 7, and 9 agonists were chosen on the basis of these agonists' previously reported synergistic effects on the immune response (Figure 1a).[15,38−40] Using these agonists, the tri-agonist would

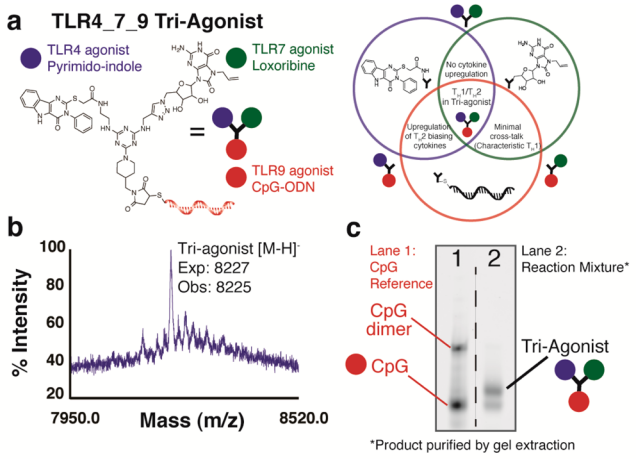

Figure 1. Schematic and characterization of tri-agonist compound, Indole_Lox_CpG. (a) Chemical structure of covalently conjugated tri-agonist compound (Indole_Lox_CpG) (left). Diagram illustrating how each TLR agonist (pyrimido-indole, loxoribine, or CpG-ODN) and the corresponding combinations (Indole_Lox, Lox_CpG, or Indole_CpG) contributed to innate immune activation (right). (b) Confirmation of synthesized Indole_Lox_CpG *via* MALDI-TOF. (c) Analysis of Indole_Lox_CpG *via* gel electrophoresis: CpG-ODN1826 reference (lane 1) and Indole_Lox_CpG reaction mixture (lane 2). Tri-agonist was extracted from the gel and isolated as purified Indole_Lox_CpG.

activate multiple signaling pathways from the endosome or from both the endosome and cell surface, instead of a single pathway, which could result in a modulated cytokine and chemokine immune response. Immune activation with our tri-agonist was determined by measurement of NF-κB activation in RAW264.7 macrophage cells (RAW-Blue) and cytokine transcription levels in bone marrow-derived dendritic cells (BMDCs). Immune cells incubated with the covalently conjugated TLR4, 7, and 9 agonists exhibited an increase in NF-κB activation and changes in cytokine expression profiles relative to a mixture of the three unconjugated agonists. Additionally, using gene expression profiling, we observed that the covalent tri-agonist displayed a shift from a characteristic T_H1 biased response (cellular response) toward a balanced response with upregulation of genes linked to a T_H2 type response (humoral/antibody response), B cell activation, and innate and adaptive immune cell recruitment. Subsequently, we used the corresponding TLR signaling inhibitors to confirm contribution from TLR4 and TLR9 activation pathways. Additional studies comparing the effect of the tri-agonist on wild-type, *MyD88*, and *TRIF* knockout mice verified activation of MyD88 and TRIF pathways, thus contributing to a synergistic increase in the immune response. Taking our studies into an *in vivo* vaccination model demonstrated that covalent conjugation of TLR agonists changes antibody production in terms of antibody breadth and depth, showing how synthetic chemical tools can shape the immune response. By chemically linking the three agonists in close proximity, we can begin to decipher how spatial arrangement contributes to immune agonist synergies at the molecular, cytokine, and gene expression levels.

RESULTS AND DISCUSSION

To covalently probe TLR synergies, we first synthesized a tri-agonist compound using three agonists exhibiting synergistic activity through specific TLRs (Scheme 1, for additional synthetic details see Schemes S1−S5). The agonists were linked using orthogonal coupling chemistries on a tri-functional small molecule core. The triazine based molecule was synthesized by treating cyanuric chloride with amines containing alkyne, amine, and maleimide functional handles.[41] Increasing the reaction temperature with the addition of each moiety resulted in a modular asymmetric core. This approach allows many three-TLR agonist combinations to be synthesized and tested in future studies.

With a core that could be conjugated to three different bioactive molecules, we attached three TLR agonists, a pyrimido[5,4-*b*]indole (Indole, TLR4 agonist), loxoribine (Lox, TLR7 agonist), and CpG-ODN1826 (CpG, TLR9 agonist) to our core.[42−46] We chose these TLR agonists based on previous studies reporting synergies activating two of the three TLRs together.[15,38−40] A pyrimido[5,4-*b*]indole compound was used to activate TLR4.[42] The carboxylic acid precursor of the pyrimido[5,4-*b*]indole compound was conjugated to the primary amine functionality on the core. Next, to activate TLR7, we attached an azide-modified loxoribine to the alkyne handle using copper-catalyzed Huisgen cycloaddition chemistry. Finally, to conjugate the TLR9 agonist CpG, the protected maleimide was revealed *via* a retro-Diels−Alder reaction and conjugated to a 5′-C6 linked thiol modified CpG-ODN1826 providing the tri-agonist conjugate, Indole_Lox_CpG (TLR4_7_9). 89.5% conversion was achieved when treating CpG with compound **9** to provide the tri-agonist, as determined by gel electrophoresis using ImageJ software. The tri-agonist was extracted from the gel and isolated as the purified tri-agonist before analysis and use. Synthesis of the tri-agonist was confirmed by MALDI-TOF and quantified *via* UV−vis spectroscopy using the fluorescent 6-FAM tag on CpG (Figures 1b, 1c, and S1). In parallel reactions, the corresponding di-agonist compounds, Indole_Lox (TLR4_7), Lox_CpG (TLR7_9), and Indole_CpG (TLR4_9), were also synthesized to determine how each agonist contributed to immune activation (Schemes S4 and S5).

First, to determine how covalent attachment of the three agonists affected synergistic activity, we measured NF-κB activation, one of the main transcription pathways involved in immune-related cytokine transcription, using the colorimetric macrophage reporter cell line, RAW-Blue. The tri- and di-agonist compounds were incubated with RAW-Blue cells for 18 h, where Indole_Lox_CpG activity (0.5 μM) was compared to

DOI: 10.1021/acscentsci.5b00274
ACS Cent. Sci. 2015, 1, 439−448

Scheme 1. Synthetic Route to Tri-agonist Indole_Lox_CpG

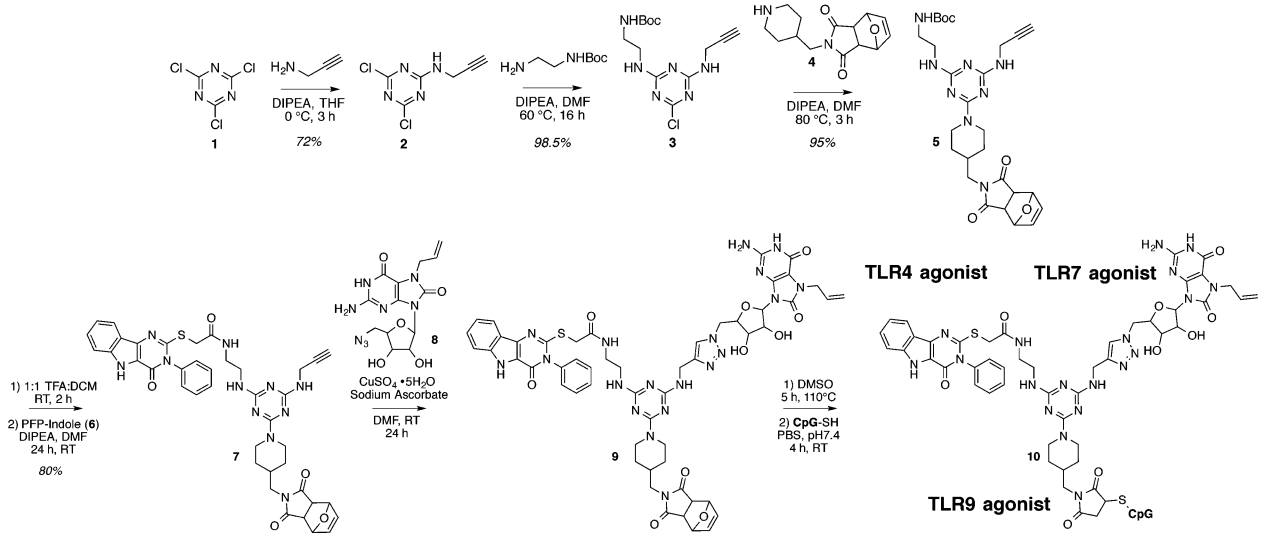

the same three TLR agonists in solution (0.5 μM Indole/0.5 μM Lox/0.5 μM CpG) as well as the related di-agonists (0.5 μM) (Figure S4 for dose response curves). For all further experiments, we used our compounds exclusively at 0.5 μM, which was the concentration at which we observed the most distinct differences in NF-κB activation (with RAW-Blue cells) and cytokine production (with bone marrow-derived dendritic cells) between tri- and di-agonist compounds.

We evaluated the differences in NF-κB activity between tri- and di-agonist constructs. Interestingly, comparing the dose response curves of Indole_Lox_CpG and Indole/Lox/CpG in RAW-Blue cells demonstrated that the linked tri-agonist and the individual agonists in solution were equipotent, but different levels of NF-κB activity were observed at 0.5 μM (Figures 2a and S4). RAW-Blue cells treated with our tri-agonist compound, Indole_Lox_CpG, exhibited a 15% increase in NF-κB activation compared to the addition of the mixture of individual agonists (Figure 2a, $*p < 0.05$). This increase in NF-κB activation was attributed to the covalent attachment between multiple TLR agonists. We hypothesized that the chemically linked agonists were presented to cells in a local manner that provided enhanced activation. Incubation with either the di-agonist compound, Lox_CpG, or CpG_core (only CpG attached to the small molecule center) resulted in a 15% decrease in NF-κB activation compared to the tri-agonist compound ($**p < 0.01$ and $***p < 0.001$, respectively). These results demonstrated how Lox (TLR7) had no effect on immune activation when conjugated to only CpG (TLR9). This observation was likely due to CpG (EC_{50}: 0.15 μM) being a more potent agonist relative to Lox (Figure S7 for loxoribine dose response curve).[43,47] In addition, we incubated RAW-Blue cells with the TLR4_9 di-agonist, while increasing the concentration of soluble Lox. We observed that at least 50 μM of soluble Lox was required to increase NF-κB activity over that elicited by just the TLR4_9 di-agonist (Figure S5, $*p < 0.05$), supporting that Lox is a weaker agonist. Therefore, Lox in the mixture of three agonists should contribute little to the overall immune activation at 0.5 μM. There was also no significant difference in NF-κB activity between Indole_Lox_CpG and the di-agonist compound Indole_CpG. This result was also likely due to the lower potency of Lox. However, Indole_CpG exhibited 27% higher NF-κB activity than CpG_core ($**p < 0.01$), showing that Indole (TLR4) contributed to an increase in CpG (TLR9) activation. These results demonstrated that treatment with covalently linked Indole_Lox_CpG activated immune cells more than the mixture of three TLR agonists at equimolar concentrations, suggesting that agonist proximity has an effect on immune activation.

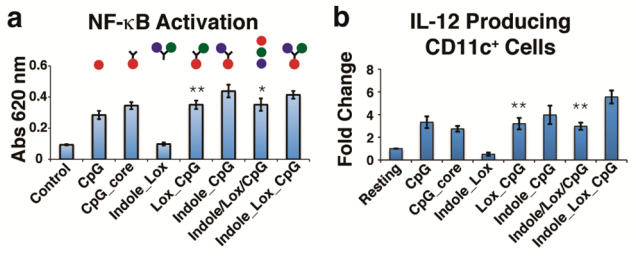

Figure 2. Innate immune activation as measured by NF-κB activity and cytokine producing dendritic cells. (a) NF-κB activation of RAW-Blue 264.7 macrophage cell line. RAW-Blue cells were treated with each compound at 0.5 μM for 18 h at 37 °C. Each figure is the result of six independent experiments, where $*p < 0.05$ and $**p < 0.01$. (b) BMDC IL-12 cytokine profile as measured by intracellular cytokine staining flow cytometry, represented as the fold change of median fluorescent intensity (MFI) of IL-12 expressing cells compared to the no agonist control. BMDCs were incubated with each compound at 0.5 μM for 6 h at 37 °C, where Brefeldin A was added for the last 4 h of incubation. Each figure represents three independent experiments, where $**p < 0.01$. All statistics represent the asterisked compound compared to Indole_Lox_CpG.

We then analyzed how our molecules affected cytokine levels by testing our compounds on primary murine bone marrow-derived dendritic cells (BMDCs). BMDCs were incubated with each compound (0.5 μM) for 6 h, and then analyzed by intracellular cytokine staining (ICS) to quantify changes in IL-12 production, a proinflammatory cytokine signature of TLR activation (Figures 2b and S8 for flow cytometry histograms).[33,48] These studies defined more subtle changes in immune activation. We observed that cells incubated with Indole_Lox_CpG exhibited a two-fold increase in the median fluorescent intensity (MFI) of IL-12 expressing cells compared to cells treated with Indole/Lox/CpG ($**p < 0.01$). These

DOI: 10.1021/acscentsci.5b00274
ACS Cent. Sci. 2015, 1, 439−448

results correlated with our RAW-Blue studies that Indole_Lox_CpG resulted in increased immune activation compared to Indole/Lox/CpG. By placing the agonists in closer proximity due to covalent conjugation, Indole_Lox_CpG possibly achieves more effective stimulation of multiple TLRs, resulting in the observed synergy. In contrast, when the three agonists are in solution, the molecules freely diffuse through the cellular environment. This diffusion could prevent localization of the TLR agonists and subsequent activation of TLR4, 7, and 9 in a spatial manner.

To further examine how each agonist contributed to immune activation, we also compared covalently conjugated di-agonist combinations that activated only two TLRs. IL-12 production of Indole_CpG, Lox_CpG, and CpG_core treated cells was comparable to that of Indole/Lox/CpG. On the other hand, Indole_Lox_CpG displayed nearly 1.5-fold higher IL-12 production than Indole_CpG, and Indole_CpG exhibited nearly 1.5-fold higher IL-12 production relative to CpG_core. Although both results were not significant, this data alluded to Lox's contribution to the upregulation of TLR activation in the tri-agonist and Indole's (TLR4) contribution to the upregulation of TLR activation when presented to immune cells with CpG (TLR9). These observations were confirmed with significant results in the gene expression profile experiments. In contrast, the activity of Lox_CpG was similar to that of CpG_core, demonstrating that Lox (TLR7) did not affect CpG (TLR9) activity and thus resulted in no change in IL-12 production. These results suggest how each agonist added to the overall activity of Indole_Lox_CpG, implying that particular agonist combinations give distinct responses.

Since these covalent synergies were suggestive of specific changes in the cytokine levels based on the covalent conjugation and agonist combinations, we examined the global influence of these two parameters on dendritic cell gene expression profiles. Using microarray gene expression profiling, we measured changes in the transcription level of 561 genes associated with an immune response using a NanoString Immunology Assay (Figure 3a, for a complete list of genes see the Supporting Information gene list spreadsheet). BMDCs were incubated with tri- and di-agonist constructs at 0.5 μM for 18 h. Then, total RNA was extracted (Qiagen RNeasy kit) and subsequently analyzed in triplicate using the microarray technology (UC Irvine Genomics High Throughput Facility). We mapped the activity of our compounds to gene expression for specific immune-related functions, such as T_H1 and T_H2 linked responses, to observe if activating specific agonist combinations in close proximity upregulated a response and to what extent. We validated that the gene expression of *Il12* agreed with our intracellular flow cytometry experiments (Figure 3c).

Additionally, we observed two main trends in the gene profile data: one in which a subset of gene expression related to T_H2 and T- and B-cell development was upregulated and a second in which a subset of gene expression related to inflammation and chemotaxis was upregulated, but to a lesser extent. The first trend corresponded to what we observed for *Il12* gene expression where Indole_Lox_CpG expressed the highest gene count, followed by Indole_CpG and last, Lox_CpG, CpG_core, and Indole/Lox/CpG, which were typically comparable (Figures 3b and 3c). This major trend of upregulation was observed not only with *Il12* expression, which is associated with a T_H1 polarized response, but also with a subset of gene expression related to T_H2 responses and

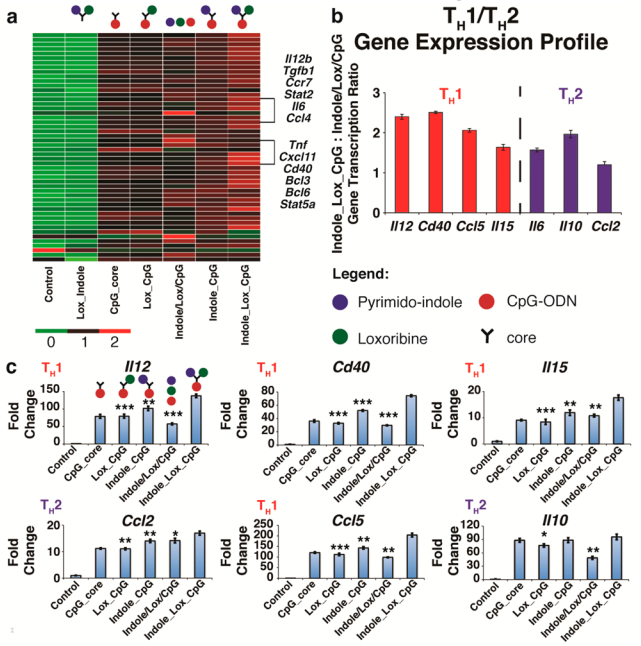

Figure 3. BMDC gene expression profile data. (a) Heat map of immune function related genes. Each figure represents the average of three independent experiments. BMDCs were incubated with each compound for 18 h at 37 °C. Total RNA was then isolated using RNeasy kit (Qiagen) and analyzed using NanoString Technology. (b) Graph illustrating T_H1/T_H2 gene expression profile comparing the gene transcription level of Indole_Lox_CpG to Indole/Lox/CpG. (c) BMDC gene profile illustrating the main trend: Indole_Lox_CpG treated cells elicited the most upregulation in a subset of gene expression. Each figure illustrates the fold change of the specified agonist compared to the no agonist control and is the result of three independent experiments, where $*p < 0.05$, $**p < 0.01$, and $***p < 0.001$. All statistics represent the asterisked compound compared to Indole_Lox_CpG.

activation of innate and adaptive immunity, which included *Il6*, *Il10*, *Il15*, *Cd40*, *Ccl2*, and *Ccl5* (Figure 3c).[49,50]

Comparing CpG_core to the di-agonists, Indole_CpG and Lox_CpG, showed that Indole (TLR4) upregulated CpG (TLR9) activity as exemplified by the 1.3-fold increase in *Il12* gene expression of Indole_CpG compared to CpG_core (Figure 3c, $**p < 0.01$). Lox (TLR7), on the other hand, did not change CpG (TLR9) activity in Lox_CpG, and Indole_Lox still did not activate immune cells. However, the addition of Lox (TLR7) to the TLR4_9 combination in Indole_Lox_CpG was associated with upregulation of the immune response expression profile. This upregulation correlated with our previous observations, signifying the importance of activating specific TLR agonist combinations in close proximity and the effect of synergistic interactions on innate immune cells.

Interestingly, Indole_Lox_CpG activity also exhibited a lower level of gene upregulation with a subset of genes compared to the agonists in solution (Figure 4). Regulatory genes and those in the TNF ligand family were upregulated to a lower degree by our covalent compound Indole_Lox_CpG compared to Indole/Lox/CpG ($**p < 0.01$). This subset of genes included *Tnfsf14*, *Tgfbi*, and *Tnfsf13b*.[51,52] In other cases, when compared to Lox_CpG, the tri-agonist compound exhibited a decrease in gene upregulation, with genes such as *Tnf* and *Ccl4* ($***p < 0.001$ and $*p < 0.05$, respectively), related to inflammation and immune cell chemoattraction. In

DOI: 10.1021/acscentsci.5b00274
ACS Cent. Sci. 2015, 1, 439−448

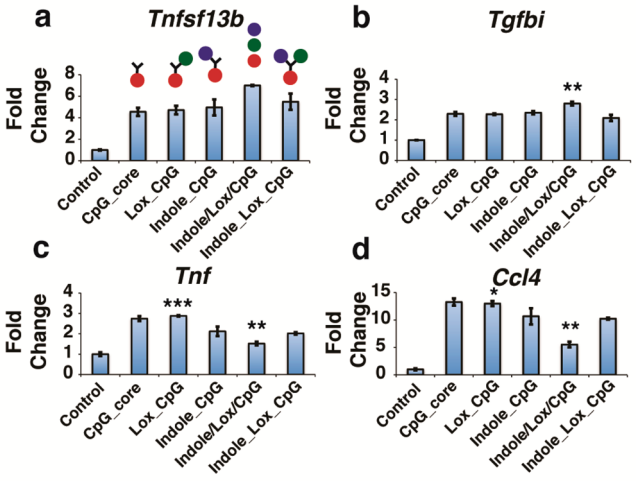

Figure 4. BMDC gene expression profile data. (a–d) BMDC gene expression profile illustrating second main trend observed, where Indole contributed to a decrease in CpG immune activity exhibited by Indole_Lox_CpG. BMDCs were incubated with each compound for 18 h at 37 °C. Total RNA was then isolated using RNeasy kit (Qiagen) and analyzed using NanoString Technology. Each figure illustrates the fold change of the specified agonist compared to the no agonist control and is the result of three independent experiments, where $*p < 0.05$, $**p < 0.01$, and $***p < 0.001$. All statistics represent the asterisked compound compared to Indole_Lox_CpG.

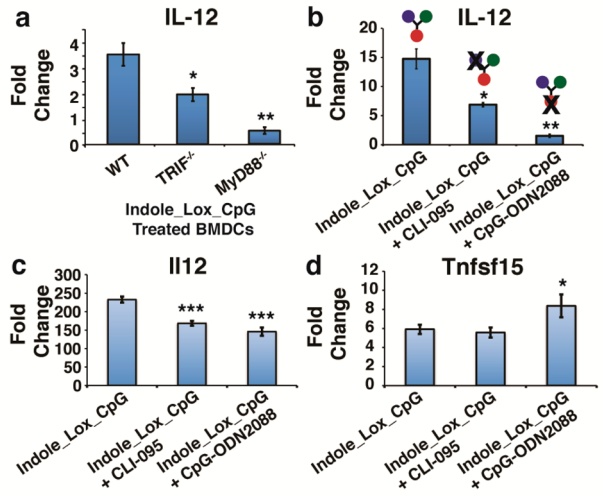

Figure 5. BMDC cytokine and gene expression profile mechanistic studies using *TRIF* and *MyD88* knockout mice or TLR signaling inhibitors. (a) IL-12 cytokine profile of wild-type (WT), *TRIF* knockout ($TRIF^{-/-}$), and *MyD88* knockout ($MyD88^{-/-}$) BMDCs treated with Indole_Lox_CpG, represented as the fold change of median fluorescent intensity (MFI) of IL-12 expressing cells compared to the no agonist control. BMDCs were incubated with Indole_Lox_CpG for 6 h at 37 °C, where Brefeldin A was added for the last 4 h of incubation. Each figure represents three independent experiments, where $*p < 0.05$ and $**p < 0.01$. (b) BMDC IL-12 cytokine profile with TLR signaling inhibitors, represented as the fold change of median fluorescent intensity (MFI) of IL-12 expressing cells compared to the no agonist control. BMDCs were incubated with the designated inhibitor for 1 h at 37 °C and then each compound for 6 h at 37 °C. Brefeldin A was added for the last 4 h of incubation. Each figure represents three independent experiments, where $*p < 0.05$ and $**p < 0.01$. (c, d) Gene expression profile representative of the two main trends observed when BMDCs were treated with TLR signaling inhibitors: (c) *Il12* expression of Indole_Lox_CpG treated cells incubated with CLI-095 (TLR4 inhibitor) and CpG-ODN2088 (TLR9 antagonist), showing contributions from TLR4 and TLR9 pathways, and (d) upregulation of gene expression profile when TLR9 signaling was inhibited. Each figure illustrates the fold change of the specified agonist compared to the no agonist control and represents three independent experiments, where $*p < 0.05$ and $***p < 0.001$. All statistics represent the asterisked compound compared to Indole_Lox_CpG.

general, this repressive trend showed that Indole_CpG and Indole_Lox_CpG exhibited lower gene expression compared to Lox_CpG and CpG_core. This result suggested that Indole (TLR4) caused less upregulation of a subset of genes related to the TNF ligand family and inflammation, which contributed to the lower fold change in gene expression observed with Indole_Lox_CpG treated cells. Comparing the tri- and di-agonist compounds demonstrated how each TLR agonist affected specific families of genes. Thus, particular agonist combinations upregulated defined subsets of gene expression to different extents, possibly affecting downstream signaling and adaptive immune responses.

To understand what signaling pathways were involved in Indole_Lox_CpG activation, we used BMDCs harvested from *MyD88* knockout ($MyD88^{-/-}$) and *TRIF* knockout ($TRIF^{-/-}$) mice. MyD88 and TRIF are adaptor proteins downstream of TLR activation and control transcription of immune-signaling molecules. Research has shown that MyD88 and TRIF work together to synergistically activate cytokine production and enhance the immune response.[30,31] We treated each group of BMDCs with Indole_Lox_CpG for 6 h and then assessed IL-12 production using ICS. When treated with the tri-agonist, both $TRIF^{-/-}$ and $MyD88^{-/-}$ BMDCs showed decreases in IL-12 production compared to treated wild-type (WT) BMDCs, nearly two-fold and seven-fold decreases ($*p < 0.05$ and $**p < 0.01$), respectively (Figure 5a). These results demonstrated that Indole_Lox_CpG activated the TRIF pathway, probably originating from Indole, since TLR4 agonists can signal *via* both MyD88 and TRIF pathways.[31,36,53] Activation was heavily dependent on MyD88 activation, as shown by the seven-fold decrease in IL-12 production, which was likely due to CpG (TLR9) being a strong MyD88 activator.[54] The difference in TRIF and MyD88 activation levels may also be due to a temporal component of immune pathway activation that will require further investigation.[12] With the ability to change MyD88 and TRIF activation levels using tri-agonist constructs, we can synthesize other multi-agonist adjuvants that potentially provide tailored immune responses.

In order to identify the precise role of each agonist/receptor set in directing BMDCs, we used a TLR inhibitor and antagonist to perform mechanistic studies. Our hypothesis was that inhibiting activation of a single type of TLR would lead to a subsequent change in cytokine levels and gene expression, confirming that receptor's role in the response elicited from Indole_Lox_CpG. A TLR4 intracellular domain inhibitor, CLI-095,[55,56] and a TLR9 antagonist oligonucleotide, CpG-ODN2088,[57] were used to selectively inhibit TLR signaling or block TLR agonist binding, respectively. The inhibitor or the antagonist was used along with the tri-agonist compound, Indole_Lox_CpG. Resulting cytokine production allowed us to determine the contribution of each agonist and TLR activation pathway.

First, we examined whether each signaling inhibitor reduced IL-12 production. BMDCs were incubated with a designated

DOI: 10.1021/acscentsci.5b00274
ACS Cent. Sci. 2015, 1, 439–448

inhibitor for 1 h before adding in Indole_Lox_CpG. The cells were then incubated for an additional 6 h, and ICS was performed to assess IL-12 production. Using CLI-095 (100 nM), a minimal, but significant, decrease in IL-12 (20% decrease of Indole_Lox_CpG IL-12 production with CLI-095 compared to Indole_Lox_CpG, $*p < 0.05$) was observed (Figures 5b and S9 for flow cytometry histograms). When incubating with CpG-ODN 2088 (100 nM), greater inhibition of IL-12 production (80% decrease of Indole_Lox_CpG IL-12 production with CpG-ODN2088 compared to Indole_Lox_CpG, $**p < 0.01$) was observed, confirming that TLR9 was the main contributor of IL-12 production when treating cells with Indole_Lox_CpG. The TLR9 antagonist, CpG-ODN2088, was used to synthesize an antagonist version of the tri-agonist compound (Indole_Lox_CpG2088). Incubating Indole_Lox_CpG2088 with BMDCs reduced IL-12 production to near resting state (Figure S10, $**p < 0.01$). The low amount of cytokine production without CpG was attributed to the potency of CpG, also showing that the incorporation of CpG was necessary to observe synergistic activity between TLR4, 7, and 9.

Expanding our studies to a broader range of cytokines and proteins *via* the NanoString assay, we analyzed gene expression of BMDCs after exposure to CLI-095 or CpG-ODN2088 and Indole_Lox_CpG (Figures 5c and 5d). We observed two main trends that correlated to the two trends observed in the previous tri- and di-agonist comparisons: first, that activation of all three receptors is important for the upregulation of genes to elicit a more balanced response, and second, that defined agonist combinations control the specific direction of the activity. The ICS experiment matched the main trend observed in the gene studies. *Il12* gene expression was reduced by CLI-095 (28% decrease of Indole_Lox_CpG *Il12* expression with CLI-095 compared to Indole_Lox_CpG, $***p < 0.001$) and further by CpG-ODN2088 (38% decrease of Indole_Lox_CpG *Il12* expression with CpG-ODN2088 compared to Indole_Lox_CpG, $***p < 0.001$), confirming contribution from TLR4 and TLR9 signaling pathways. This trend applied to the majority of genes, including proinflammatory genes *Il6* and *Il15* as well as adaptive immune-related genes *Ccl2* and *Ccl5*. The second trend observed resulted in gene upregulation relative to Indole_Lox_CpG when TLR9 inhibition occurred and minimal to no decrease in gene expression with TLR4 inhibition. This was observed for genes related to $CD4^+$ cell chemotaxis and development as well as the TNF ligand family. This confirmed how close agonist proximity through covalent modifications resulted in contribution from multiple TLR activation pathways, which altered and directed innate immune responses.

After studying how our compounds changed the immune response *in vitro*, we wanted to observe how Indole_Lox_CpG performed *in vivo* using a model vaccination system, vaccinia virus (small pox). C57BL/6 mice were immunized *via* im injection with heat-inactivated vaccinia virus (2.5×10^7 pfu/mL) and adjuvanted with either phosphate buffered saline (PBS) as the vehicle, Indole/Lox/CpG (0.05 nmol of each agonist), or Indole_Lox_CpG (0.05 nmol). Mice were boosted on day 14 with the designated vaccine. Serum was drawn from the mice on day 0, 7, 14, 21, and 28, and analyzed using a vaccinia protein microarray[58] to determine antibody depth and breadth. Looking at the immunodominant vaccinia antigen (WR148), Indole_Lox_CpG displayed the greatest depth in IgG1 antibody response (Figure 6a). Additionally, Indole_Lox_CpG elicited the broadest breadth in antigen-specific

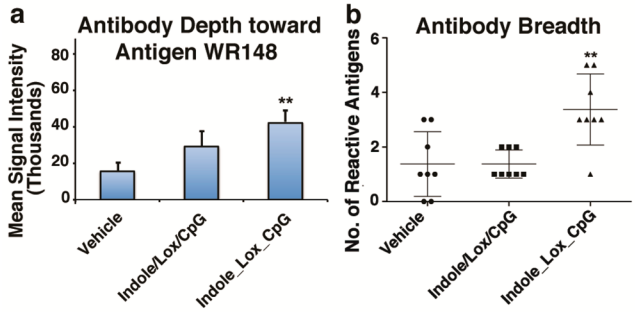

Figure 6. Effect of Indole_Lox_CpG on IgG1 immune response in heat-inactivated vaccinia virus immunized mice. Mice were vaccinated *via* im injection on day 0 with heat inactivated vaccinia virus (2.5×10^7 pfu/mL) adjuvanted with PBS (Vehicle), Indole/Lox/CpG, or Indole_Lox_CpG with a total injection volume of 50 μL. Mice were boosted on day 14. At day 28, the experiment end point, serum was collected from mice and probed on a vaccinia protein microarray. (a) Mean signal intensities of sera toward vaccinia immunodominant antigen WR148 at day 28, where $**p < 0.01$. (b) Number of reactive antigens in sera of immunized mice at day 28, where $**p < 0.01$. Results are expressed as mean ± SEM; $n = 8$/group; unpaired, two-tailed *t* test. All statistics represent the asterisked compound compared to the no adjuvant vehicle.

antibody response compared to the no adjuvant vehicle or Indole/Lox/CpG (Figure 6b, $**p < 0.01$). In contrast, Indole/Lox/CpG did not significantly change antibody depth or breadth compared to the vehicle. These results demonstrated that delivering a single, spatially defined tri-agonist compound *in vivo* can control antibody responses. The difference in antibody response between the tri-agonist, Indole_Lox_CpG, and Indole/Lox/CpG may be attributed to the different immune signaling pathways that are activated and the order in which the TLRs are stimulated, as a result of the covalent linkage and spatial arrangement of the TLR agonists. We are currently working on performing more *in vivo* studies to understand the mechanism and effect of different agonist combinations. These experiments show the utility and influence covalently linked multi-agonists might have on immunotherapy development.

CONCLUSIONS

Here, we present evidence that the spatial arrangement of TLR agonists and the specific combinations of stimulated receptors resulted in defined activation patterns of dendritic cells. We detailed the synthesis of a tri-agonist construct, expanding recent two agonist synergistic studies to the use of three agonists. Through conjugation of a third agonist and in close proximity, we created a distinctive, more balanced response, shifting the immune response from T_H1 polarization to a more balanced T_H1/T_H2 response and activation of innate and adaptive immunity. By comparing the tri-agonist compound to di-agonist constructs, we observed how each agonist shaped the innate immune response. Mechanistic studies were performed with adaptor protein knockout mice and the corresponding TLR inhibitor and antagonist to show the specific receptors and pathways through which the tri-agonist compound proceeded. We also observed that Indole_Lox_CpG increased antibody breadth and signal intensity toward a specific antigen when compared to the mixture of three agonists. In future studies, we plan to synthesize other TLR agonist combinations. These molecules will aid in determining how covalent synergies direct

DOI: 10.1021/acscentsci.5b00274
ACS Cent. Sci. 2015, 1, 439−448

antigen presentation and the types of cell populations that become activated. The covalently linked Indole_Lox_CpG aided in elucidating how TLR4, 7, and 9 synergies contributed to the observed changes in innate immune responses. Chemically controlling the spatial organization of innate immune agonists and specific agonist combinations can be used as a tool to direct immune responses and further understand how the immune system responds to pathogens. From this, researchers can potentially start to develop more effective immunotherapies using adjuvants designed to elicit targeted responses.

METHODS

General Materials and Methods. Reagents were purchased from Sigma-Aldrich and used as is unless otherwise noted. Single stranded CpG-ODN1826 (Thio-C6-5′-TCCAT-GACGTTCCTGACGTT-3′-6-FAM) with a phosphorothioated backbone was purchased from IDT. Centrifugal Filter Devices (3k) and ZipTip$_{C18}$ for MALDI-MS were purchased from Millipore. Compounds were filtered using 0.22 μM syringe filters (Restek). Anti-mouse antibodies CD16/32 (93), APC anti-mouse IL-12 (C15.6), and Rat Isotype IgG1 (RTK2071) were purchased from BioLegend. BD Cytofix/Cytoperm Kit for intracellular cytokine flow cytometry and GolgiPlug were purchased from BD Biosciences. Bone marrow-derived dendritic cells (BMDCs) were harvested from 6-week-old C57BL/6, B6.129P2(SJL)-*Myd88*$^{tm1.1Defr}$/J (*MyD88*$^{-/-}$), and C57BL/6J-*Ticam1*^{Lps2}/J (*TRIF*$^{-/-}$) mice (Jackson Laboratory). BMDCs were cultured in BMDC primary medium: RPMI 1640 (Life Technologies), 10% heat inactivated fetal bovine serum (FBS), 20 ng/mL granulocyte-macrophage colony-stimulating factor (GM-CSF) (produced from "66" cell line), 2 mM L-glutamine (Life Technologies), antibiotic-antimycotic (1×) (Life Technologies), and 50 μM beta-mercaptoethanol (all components were 0.2 μM sterile filtered together before use). RAW264.7 macrophage cells (RAW-Blue) were cultured in D-MEM High Glucose medium (Life Technologies), 10% FBS, 2 mM L-glutamine, 200 μg/mL Zeocin (InvivoGen), and antibiotic-antimycotic (1×). Experiments were run in D-MEM High Glucose medium (Life Technologies), 10% heat inactivated FBS, 2 mM L-glutamine, and antibiotic-antimycotic (1×). Sterile phosphate buffered saline (PBS) buffer was obtained from Life Technologies. Fluorescence-activated cell sorting (FACS) buffer contained PBS (1×), 10% FBS, and 0.1% sodium azide. Mass spectra were obtained using MALDI-TOF (AB SCIEX TOF/TOF 5800). Flow cytometry data was acquired using a BD Accuri C6 Flow Cytometer and analyzed using the BD Accuri C6 software. RAW-Blue absorbances were measured on a Fisher Scientific MultiSkan FC. UV−vis spectra were obtained using NanoDrop 2000c spectrophotometer. Gel images were obtained using a GE Typhoon scanner. ImageJ was used to quantify percent conversion of the tri-agonist. Total RNA isolation was performed using an RNeasy Kit (Qiagen), according to the provided manufacturer's instructions. Total RNA samples were analyzed by the UC Irvine Genomics High Throughput Facilities using a NanoString Immunology Assay (NanoString Technologies) to obtain gene expression profiles. Semi-preparative high performance liquid chromatography was performed on a 1260 Infinity HPLC (Agilent). Gel electrophoresis was carried out using 10% TBE-urea gels in a Mini-PROTEAN tetra cell (BIO-RAD). All animal studies and mice maintenance were approved by the Institutional Animal Care and Use Committee (IACUC). Data was analyzed using a two-tailed *t* test. All values were reported as mean ± SD, unless stated otherwise.

RAW264.7 Macrophage (RAW-Blue) NF-κB Assay. RAW-Blue cells were plated at 55 × 10^4 cells/mL density (180 μL) in 96-well plates using testing media as described in General Materials and Methods. RAW-Blue cells were incubated with 20 μL of each agonist for 18 h at 37 °C in a CO_2 incubator. Cell medium (50 μL) from the stimulated RAW-Blue cells was removed, placed into a 96-well plate, and incubated with QUANTI-Blue solution (InvivoGen) (150 μL) for 1−5 h at 37 °C in a CO_2 incubator. The absorbance (620 nm) was measured using a Fisher Scientific MultiSkan FC.

***In Vitro* Bone Marrow-Derived Dendritic Cell Culture and Intracellular Cytokine Staining.** Monocytes were harvested from 6-week-old C57BL/6, B6.129P2(SJL)-*Myd88*$^{tm1.1Defr}$/J (*MyD88*$^{-/-}$), or C57BL/6J-*Ticam1*^{Lps2}/J (*TRIF*$^{-/-}$) mice.[59] Monocytes were differentiated into dendritic cells (BMDCs) using supplemented culture medium: RPMI 1640 (Life Technologies), 10% heat inactivated fetal bovine serum (Sigma), 20 ng/mL granulocyte-macrophage colony-stimulating factor (produced using "66" cell line), 2 mM L-glutamine (Life Technologies), antibiotic-antimycotic (1×) (Life Technologies), and 50 μM beta-mercaptoethanol (Sigma). After 5 days of culture, BMDCs were incubated with each agonist (0.5 μM) in culture medium for 6 h at 37 °C in a CO_2 incubator. GolgiPlug (BD Biosciences), containing Brefeldin A, was added to cell culture for the final 4 h of culture. Cells were stained for intracellular IL-12 cytokine production and analyzed using BD Accuri C6.

Immunization. C57BL/6 mice were vaccinated intramuscularly (im) at day 0 with heat-inactivated vaccinia virus Western Reserve (VVWR) strain (2.5 × 10^7 pfu/mL) adjuvanted with specified multi-agonist compound(s) (0.05 nmol) or PBS as a control in a total injection volume of 50 μL. Mice received vaccine boost at day 14. Serum samples were collected from mice *via* saphenous vein at day 0, 7, 14, 21, and 28 postvaccination.

Viruses. VVWR stocks were grown on HeLa cells in T175 flasks, infecting at a multiplicity of infection of 0.5. Cells were harvested at 60 h, and virus was isolated by rapidly freeze−thawing the cell pellet three times in a volume of 2.3 mL of RPMI plus 1% fetal calf serum (FCS). Cell debris was removed by centrifugation. Clarified supernatant was frozen at −80 °C as virus stock. VVWR stocks were titered on Vero cells (2 × 10^8 pfu/mL). Heat-inactivated VVWR stock was prepared by incubating virus on a water bath at 65 °C for 1 h.

Gel Electrophoresis. CpG-ODN containing compounds were purified using Mini-PROTEAN TBE-Urea Precast Gels (BIO-RAD) and Mini-PROTEAN Tetra Cell system. Compounds were loaded into gels in TBE urea buffer (7:20 compound:loading buffer). Gels were run in TBE buffer at 100 V for 1 h. The resulting gels were imaged using a GE Typhoon gel scanner. The desired band was excised, crushed, and eluted into HPLC grade water overnight at 37 °C. The resulting solution was concentrated using 3k Amicon Centrifugal Filter Units (EMD Millipore) and filtered using 0.2 μM cellulose acetate syringe filter (Restek). The resulting product was desalted using ZipTip$_{C18}$, analyzed by MALDI-TOF using 3-hydroxypicolinic acid matrix, and quantified using a NanoDrop spectrophotometer.

MALDI-TOF. The reaction mixture was passed through ZipTip$_{C18}$ (Millipore) according to Millipore protocol:

DOI: 10.1021/acscentsci.5b00274
ACS Cent. Sci. 2015, 1, 439−448

$ZipTip_{C18}$ was equilibrated with 50% acetonitrile/water (2 × 10 μL) and subsequently 0.1 M triethylammonium acetate (TEAA) (3 × 10 μL). The oligonucleotide-containing compound was passed through the $ZipTip_{C18}$ (10 × 10 μL). The $ZipTip_{C18}$ was washed with 0.1 M TEAA buffer (3 × 10 μL) followed by nanopure water (3 × 10 μL). The desired product was eluted using 50% acetonitrile/water (3 × 10 μL). The eluted product was concentrated using a speed-vacuum and mixed with 0.36 M 3-hydroxypicolinic acid matrix (1:1 acetonitrile:300 mM ammonium citrate solution in 50% acetonitrile/water) (2 μL). The sample was spotted directly onto the MALDI plate and analyzed in negative ion mode. For small molecules, the sample was spotted with α-cyano-4-hydroxycinnamic acid matrix (in 1:1 acetonitrile:water with 0.1% TFA) and analyzed in positive ion mode.

Production and Probing of Vaccinia Protein Microarray. The cloning and expression platform is described in detail previously.[58] Briefly, custom PCR primers comprising 20 bp of gene-specific sequence with 33 bp of "adapter" sequences were used in PCRs with vaccinia virus WR strain genomic DNA as a template. The adapter sequences, which become incorporated into the termini flanking the amplified gene, were homologous to the cloning site of the T7 expression vector pNHisCHA (Gene Therapy Systems, San Diego, CA) and allowed the PCR products to be cloned by homologous recombination in competent DH5α cells. The adapters also incorporated a 5′-polyhistidine epitope, an ATG translation start codon, and a 3′-hemagglutinin epitope and T7 terminator. Sequence-confirmed plasmids were expressed in 5 h *in vitro* transcription-translation reactions (RTS 100 kits from Roche) according to the manufacturer's instructions. Protein expression was monitored either by dot blot or by microarray using both monoclonal anti-polyhistidine (clone His-1 from Sigma) and monoclonal anti-hemagglutinin (clone 3F10 from Roche) antibodies, followed by appropriate secondary antibodies. Microarrays were printed onto nitrocellulose coated glass slides (FAST from Schleicher & Schuell Bioscience) using an Omni Grid 100 microarray printer (Gene Machines). Prior to array staining, the sera were diluted to 1/100 in Protein Array Blocking Buffer (Schleicher & Schuell Bioscience) containing *Escherichia coli* lysate at a final concentration of 10% and incubated at room temperature for 1 h with constant mixing. The arrays were rehydrated in blocking buffer for 30 min and probed with the pretreated sera for 2 h at room temperature with constant agitation. The slides were then washed 3 times in Tris buffer containing 0.05% Tween-20 and incubated with biotin conjugated anti-mouse IgG1 secondary antibodies at 1:200 in blocking buffer for 1 h. The slides were then washed 3 times with Tris buffer containing 0.05% Tween-20 followed by incubation with streptavidin-Surelight P-3 conjugated at 1:200 in blocking buffer for 45 min. After washing, the slides were air-dried under brief centrifugation and stored in a desiccator at room temperature. The microarrays were scanned using a Gene Pix 4100A scanner (Molecular Devices, Sunnyvale, CA), and image analysis was performed with Genepix Pro 5.0 software (Molecular Devices). The spot intensity was calculated as the median spot value minus local spot background. A secondary correction for background binding to *E. coli* proteins in the reaction mixture was done by subtracting an average of the no-DNA spots from the background-corrected spot value.

■ ASSOCIATED CONTENT

Supporting Information

The Supporting Information is available free of charge on the ACS Publications website at DOI: 10.1021/acscentsci.5b00274.

Synthetic protocols and schemes and *in vitro* cell data (PDF)

Gene list (XLSX)

■ AUTHOR INFORMATION

Corresponding Author

*E-mail: aesserka@uci.edu.

Notes

The authors declare no competing financial interest.

■ ACKNOWLEDGMENTS

This work was supported by the UC Irvine Department of Chemistry, the NIH (DP2-AI112194), the Hellman Family Foundation, the National Science Foundation Graduate Research Fellowship under Grant No. DGE-0808392 (awarded to J.K.T.), the UC Irvine Undergraduate Research Opportunities Program (UROP) Fellowship (awarded to H.Y.W), the NIAID U01 AI078213 (awarded to P.L.F.), and 2R44AI058365 (awarded to D.H.D.). We would like to thank Drs. John Greaves and Beniam Berhane for assistance with mass spectrometry and the UC Irvine Genomics High Throughput Facility for NanoString Immunology Panel RNA analysis.

■ REFERENCES

(1) Schreibelt, G.; Benitez-Ribas, D.; Schuurhuis, D.; Lambeck, A. J. A.; van Hout-Kuijer, M.; Schaft, N.; Punt, C. J. A.; Figdor, C. G.; Adema, G. J.; de Vries, I. J. M. Commonly Used Prophylactic Vaccines as an Alternative for Synthetically Produced TLR Ligands to Mature Monocyte-Derived Dendritic Cells. *Blood* **2010**, *116* (4), 564−574.

(2) Taub, D. D.; Ershler, W. B.; Janowski, M.; Artz, A.; Key, M. L.; McKelvey, J.; Muller, D.; Moss, B.; Ferrucci, L.; Duffey, P. L.; et al. Immunity from Smallpox Vaccine Persists for Decades: A Longitudinal Study. *Am. J. Med.* **2008**, *121* (12), 1058−1064.

(3) Garcia-Cordero, J. L.; Nembrini, C.; Stano, A.; Hubbell, J. A.; Maerkl, S. J. A High-Throughput Nanoimmunoassay Chip Applied to Large-Scale Vaccine Adjuvant Screening. *Integr. Biol. Quant. Biosci. Nano Macro* **2013**, *5* (4), 650−658.

(4) Trinchieri, G.; Sher, A. Cooperation of Toll-like Receptor Signals in Innate Immune Defence. *Nat. Rev. Immunol.* **2007**, *7* (3), 179−190.

(5) Coffman, R. L.; Sher, A.; Seder, R. A. Vaccine Adjuvants: Putting Innate Immunity to Work. *Immunity* **2010**, *33* (4), 492−503.

(6) Steinhagen, F.; Kinjo, T.; Bode, C.; Klinman, D. M. TLR-Based Immune Adjuvants. *Vaccine* **2011**, *29* (17), 3341−3355.

(7) Kaufmann, S. H. E. The Contribution of Immunology to the Rational Design of Novel Antibacterial Vaccines. *Nat. Rev. Microbiol.* **2007**, *5* (7), 491−504.

(8) Reed, S. G.; Orr, M. T.; Fox, C. B. Key Roles of Adjuvants in Modern Vaccines. *Nat. Med.* **2013**, *19* (12), 1597−1608.

(9) Bergmann-Leitner, E. S.; Leitner, W. W. Adjuvants in the Driver's Seat: How Magnitude, Type, Fine Specificity and Longevity of Immune Responses Are Driven by Distinct Classes of Immune Potentiators. *Vaccines* **2014**, *2* (2), 252−296.

(10) Wu, T. Y.-H.; Singh, M.; Miller, A. T.; Gregorio, E. D.; Doro, F.; D'Oro, U.; Skibinski, D. A. G.; Mbow, M. L.; Bufali, S.; Herman, A. E.; et al. Rational Design of Small Molecules as Vaccine Adjuvants. *Sci. Transl. Med.* **2014**, *6* (263), 263ra160−ra263ra160.

(11) Santone, M.; Aprea, S.; Wu, T. Y.-H.; Cooke, M. P.; Mbow, M. L.; Valiante, N. M.; Rush, J. S.; Dougan, S.; Avalos, A.; Ploegh, H.; et al. A New TLR2 Agonist Promotes Cross-Presentation by Mouse and Human Antigen Presenting Cells. *Hum. Vaccines Immunother.* **2015**, *11* (8), 2038−2050.

DOI: 10.1021/acscentsci.5b00274
ACS Cent. Sci. 2015, 1, 439−448

(12) Napolitani, G.; Rinaldi, A.; Bertoni, F.; Sallusto, F.; Lanzavecchia, A. Selected Toll-like Receptor Agonist Combinations Synergistically Trigger a T Helper Type 1-Polarizing Program in Dendritic Cells. *Nat. Immunol.* **2005**, *6* (8), 769−776.
(13) Honda, K.; Ohba, Y.; Yanai, H.; Negishi, H.; Mizutani, T.; Takaoka, A.; Taya, C.; Taniguchi, T. Spatiotemporal Regulation of MyD88−IRF-7 Signalling for Robust Type-I Interferon Induction. *Nature* **2005**, *434* (7036), 1035−1040.
(14) Ghosh, T. K.; Mickelson, D. J.; Solberg, J. C.; Lipson, K. E.; Inglefield, J. R.; Alkan, S. S. TLR−TLR Cross Talk in Human PBMC Resulting in Synergistic and Antagonistic Regulation of Type-1 and 2 Interferons, IL-12 and TNF-α. *Int. Immunopharmacol.* **2007**, *7* (8), 1111−1121.
(15) Kasturi, S. P.; Skountzou, I.; Albrecht, R. A.; Koutsonanos, D.; Hua, T.; Nakaya, H. I.; Ravindran, R.; Stewart, S.; Alam, M.; Kwissa, M.; et al. Programming the Magnitude and Persistence of Antibody Responses with Innate Immunity. *Nature* **2011**, *470* (7335), 543−547.
(16) Fox, C. B.; Sivananthan, S. J.; Duthie, M. S.; Vergara, J.; Guderian, J. A.; Moon, E.; Coblentz, D.; Reed, S. G.; Carter, D. A Nanoliposome Delivery System to Synergistically Trigger TLR4 AND TLR7. *J. Nanobiotechnol.* **2014**, *12* (1), 17.
(17) Goff, P. H.; Hayashi, T.; Martínez-Gil, L.; Corr, M.; Crain, B.; Yao, S.; Cottam, H. B.; Chan, M.; Ramos, I.; Eggink, D.; et al. Synthetic Toll-Like Receptor 4 (TLR4) and TLR7 Ligands as Influenza Virus Vaccine Adjuvants Induce Rapid, Sustained, and Broadly Protective Responses. *J. Virol.* **2015**, *89* (6), 3221−3235.
(18) Shinchi, H.; Crain, B.; Yao, S.; Chan, M.; Zhang, S. S.; Ahmadiiveli, A.; Suda, Y.; Hayashi, T.; Cottam, H. B.; Carson, D. Enhancement of the Immunostimulatory Activity of a TLR7 Ligand by Conjugation to Polysaccharides. *Bioconjugate Chem.* **2015**, *26* (8), 1713−1723.
(19) Wiley, S. R.; Raman, V. S.; Desbien, A.; Bailor, H. R.; Bhardwaj, R.; Shakri, A. R.; Reed, S. G.; Chitnis, C. E.; Carter, D. Targeting TLRs Expands the Antibody Repertoire in Response to a Malaria Vaccine. *Sci. Transl. Med.* **2011**, *3* (93), 93ra69−ra93ra69.
(20) Liu, H.; Irvine, D. J. Guiding Principles in the Design of Molecular Bioconjugates for Vaccine Applications. *Bioconjugate Chem.* **2015**, *26* (5), 791−801.
(21) Liu, H.; Moynihan, K. D.; Zheng, Y.; Szeto, G. L.; Li, A. V.; Huang, B.; Van Egeren, D. S.; Park, C.; Irvine, D. J. Structure-Based Programming of Lymph-Node Targeting in Molecular Vaccines. *Nature* **2014**, *507* (7493), 519−522.
(22) O'Hagan, D. T.; Fox, C. B. Are We Entering a New Age for Human Vaccine Adjuvants? *Expert Rev. Vaccines* **2015**, *14* (7), 909−911.
(23) De Geest, B. G.; Willart, M. A.; Lambrecht, B. N.; Pollard, C.; Vervaet, C.; Remon, J. P.; Grooten, J.; De Koker, S. Surface-Engineered Polyelectrolyte Multilayer Capsules: Synthetic Vaccines Mimicking Microbial Structure and Function. *Angew. Chem., Int. Ed.* **2012**, *51* (16), 3862−3866.
(24) Mancini, R. J.; Tom, J. K.; Esser-Kahn, A. P. Covalently Coupled Immunostimulant Heterodimers. *Angew. Chem., Int. Ed.* **2014**, *53* (1), 189−192.
(25) Pavot, V.; Rochereau, N.; Rességuier, J.; Gutjahr, A.; Genin, C.; Tiraby, G.; Perouzel, E.; Lioux, T.; Vernejoul, F.; Verrier, B.; et al. Cutting Edge: New Chimeric NOD2/TLR2 Adjuvant Drastically Increases Vaccine Immunogenicity. *J. Immunol.* **2014**, *193* (12), 5781−5785.
(26) Shukla, N. M.; Mutz, C. A.; Malladi, S. S.; Warshakoon, H. J.; Balakrishna, R.; David, S. A. Toll-Like Receptor (TLR)-7 and −8 Modulatory Activities of Dimeric Imidazoquinolines. *J. Med. Chem.* **2012**, *55* (3), 1106−1116.
(27) Shukla, N. M.; Salunke, D. B.; Balakrishna, R.; Mutz, C. A.; Malladi, S. S.; David, S. A. Potent Adjuvanticity of a Pure TLR7-Agonistic Imidazoquinoline Dendrimer. *PLoS One* **2012**, *7* (8), e43612.
(28) Querec, T.; Bennouna, S.; Alkan, S.; Laouar, Y.; Gorden, K.; Flavell, R.; Akira, S.; Ahmed, R.; Pulendran, B. Yellow Fever Vaccine YF-17D Activates Multiple Dendritic Cell Subsets *via* TLR2, 7, 8, and 9 to Stimulate Polyvalent Immunity. *J. Exp. Med.* **2006**, *203* (2), 413−424.
(29) Pulendran, B. Learning Immunology from the Yellow Fever Vaccine: Innate Immunity to Systems Vaccinology. *Nat. Rev. Immunol.* **2009**, *9* (10), 741−747.
(30) Bagchi, A.; Herrup, E. A.; Warren, H. S.; Trigilio, J.; Shin, H.-S.; Valentine, C.; Hellman, J. MyD88-Dependent and MyD88-Independent Pathways in Synergy, Priming, and Tolerance between TLR Agonists. *J. Immunol.* **2007**, *178* (2), 1164−1171.
(31) Ouyang, X.; Negishi, H.; Takeda, R.; Fujita, Y.; Taniguchi, T.; Honda, K. Cooperation between MyD88 and TRIF Pathways in TLR Synergy *via* IRF5 Activation. *Biochem. Biophys. Res. Commun.* **2007**, *354* (4), 1045−1051.
(32) Ting Tan, R. S.; Lin, B.; Liu, Q.; Tucker-Kellogg, L.; Ho, B.; Leung, B. P. L.; Ding, J. L. The Synergy in Cytokine Production through MyD88-TRIF Pathways Is Co-Ordinated with ERK Phosphorylation in Macrophages. *Immunol. Cell Biol.* **2013**, *91* (5), 377−387.
(33) Krummen, M.; Balkow, S.; Shen, L.; Heinz, S.; Loquai, C.; Probst, H.-C.; Grabbe, S. Release of IL-12 by Dendritic Cells Activated by TLR Ligation Is Dependent on MyD88 Signaling, Whereas TRIF Signaling Is Indispensable for TLR Synergy. *J. Leukocyte Biol.* **2010**, *88* (1), 189−199.
(34) Kwissa, M.; Nakaya, H. I.; Oluoch, H.; Pulendran, B. Distinct TLR Adjuvants Differentially Stimulate Systemic and Local Innate Immune Responses in NonHuman Primates. *Blood* **2012**, *119* (9), 2044−2055.
(35) Pulendran, B. Modulating Vaccine Responses with Dendritic Cells and Toll-like Receptors. *Immunol. Rev.* **2004**, *199* (1), 227−250.
(36) O'Neill, L. A. J.; Golenbock, D.; Bowie, A. G. The History of Toll-like Receptors — Redefining Innate Immunity. *Nat. Rev. Immunol.* **2013**, *13* (6), 453−460.
(37) Kagan, J. C.; Su, T.; Horng, T.; Chow, A.; Akira, S.; Medzhitov, R. TRAM Couples Endocytosis of Toll-like Receptor 4 to the Induction of Interferon-β. *Nat. Immunol.* **2008**, *9* (4), 361−368.
(38) De Nardo, D.; De Nardo, C. M.; Nguyen, T.; Hamilton, J. A.; Scholz, G. M. Signaling Crosstalk during Sequential TLR4 and TLR9 Activation Amplifies the Inflammatory Response of Mouse Macrophages. *J. Immunol.* **2009**, *183* (12), 8110−8118.
(39) Moody, M. A.; Santra, S.; Vandergrift, N. A.; Sutherland, L. L.; Gurley, T. C.; Drinker, M. S.; Allen, A. A.; Xia, S.-M.; Meyerhoff, R. R.; Parks, R.; et al. Toll-like Receptor 7/8 (TLR7/8) and TLR9 Agonists Cooperate to Enhance HIV-1 Envelope Antibody Responses in Rhesus Macaques. *J. Virol.* **2014**, *88* (6), 3329−3339.
(40) Theiner, G.; Rössner, S.; Dalpke, A.; Bode, K.; Berger, T.; Gessner, A.; Lutz, M. B. TLR9 Cooperates with TLR4 to Increase IL-12 Release by Murine Dendritic Cells. *Mol. Immunol.* **2008**, *45* (1), 244−252.
(41) Banerjee, R.; Pace, N. J.; Brown, D. R.; Weerapana, E. 1,3,5-Triazine as a Modular Scaffold for Covalent Inhibitors with Streamlined Target Identification. *J. Am. Chem. Soc.* **2013**, *135* (7), 2497−2500.
(42) Chan, M.; Hayashi, T.; Mathewson, R. D.; Nour, A.; Hayashi, Y.; Yao, S.; Tawatao, R. I.; Crain, B.; Tsigelny, I. F.; Kouznetsova, V. L.; et al. Identification of Substituted Pyrimido[5,4-B]indoles as Selective Toll-Like Receptor 4 Ligands. *J. Med. Chem.* **2013**, *56* (11), 4206−4223.
(43) Heil, F.; Ahmad-Nejad, P.; Hemmi, H.; Hochrein, H.; Ampenberger, F.; Gellert, T.; Dietrich, H.; Lipford, G.; Takeda, K.; Akira, S.; et al. The Toll-like Receptor 7 (TLR7)-Specific Stimulus Loxoribine Uncovers a Strong Relationship within the TLR7, 8 and 9 Subfamily. *Eur. J. Immunol.* **2003**, *33* (11), 2987−2997.
(44) Krieg, A. M. The Role of CpG Motifs in Innate Immunity. *Curr. Opin. Immunol.* **2000**, *12* (1), 35−43.
(45) Vollmer, J.; Krieg, A. M. Immunotherapeutic Applications of CpG Oligodeoxynucleotide TLR9 Agonists. *Adv. Drug Delivery Rev.* **2009**, *61* (3), 195−204.
(46) Vollmer, J.; Weeratna, R.; Payette, P.; Jurk, M.; Schetter, C.; Laucht, M.; Wader, T.; Tluk, S.; Liu, M.; Davis, H. L.; et al.

DOI: 10.1021/acscentsci.5b00274
ACS Cent. Sci. 2015, 1, 439−448

Characterization of Three CpG Oligodeoxynucleotide Classes with Distinct Immunostimulatory Activities. *Eur. J. Immunol.* **2004**, *34* (1), 251−262.
(47) Liu, J.; Xu, C.; Liu, Y.-L.; Matsuo, H.; Hsieh, R. P.; Lo, J.-F.; Tseng, P.-H.; Yuan, C.-J.; Luo, Y.; Xiang, R.; et al. Activation of Rabbit TLR9 by Different CpG-ODN Optimized for Mouse and Human TLR9. *Comp. Immunol. Microbiol. Infect. Dis.* **2012**, *35* (5), 443−451.
(48) Mitchell, D.; Yong, M.; Raju, J.; Willemsen, N.; Black, M.; Trent, A.; Tirrell, M.; Olive, C. Toll-like Receptor-Mediated Adjuvanticity and Immunomodulation in Dendritic Cells: Implications for Peptide Vaccines. *Hum. Vaccines* **2011**, *7* (0), 85−93.
(49) Gu, L.; Tseng, S.; Horner, R. M.; Tam, C.; Loda, M.; Rollins, B. J. Control of TH2 Polarization by the Chemokine Monocyte Chemoattractant Protein-1. *Nature* **2000**, *404* (6776), 407−411.
(50) Ouyang, W.; Rutz, S.; Crellin, N. K.; Valdez, P. A.; Hymowitz, S. G. Regulation and Functions of the IL-10 Family of Cytokines in Inflammation and Disease. *Annu. Rev. Immunol.* **2011**, *29* (1), 71−109.
(51) Menten, P.; Wuyts, A.; Van Damme, J. Macrophage Inflammatory Protein-1. *Cytokine Growth Factor Rev.* **2002**, *13* (6), 455−481.
(52) Collette, Y.; Gilles, A.; Pontarotti, P.; Olive, D. A Co-Evolution Perspective of the TNFSF and TNFRSF Families in the Immune System. *Trends Immunol.* **2003**, *24* (7), 387−394.
(53) Orr, M. T.; Duthie, M. S.; Windish, H. P.; Lucas, E. A.; Guderian, J. A.; Hudson, T. E.; Shaverdian, N.; O'Donnell, J.; Desbien, A. L.; Reed, S. G.; et al. MyD88 and TRIF Synergistic Interaction Is Required for TH1-Cell Polarization with a Synthetic TLR4 Agonist Adjuvant. *Eur. J. Immunol.* **2013**, *43* (9), 2398−2408.
(54) Hacker, G.; Redecke, V.; Hacker, H. Activation of the Immune System by Bacterial CpG-DNA. *Immunology* **2002**, *105* (3), 245−251.
(55) Kawamoto, T.; Ii, M.; Kitazaki, T.; Iizawa, Y.; Kimura, H. TAK-242 Selectively Suppresses Toll-like Receptor 4-Signaling Mediated by the Intracellular Domain. *Eur. J. Pharmacol.* **2008**, *584* (1), 40−48.
(56) Takashima, K.; Matsunaga, N.; Yoshimatsu, M.; Hazeki, K.; Kaisho, T.; Uekata, M.; Hazeki, O.; Akira, S.; Iizawa, Y.; Ii, M. Analysis of Binding Site for the Novel Small-Molecule TLR4 Signal Transduction Inhibitor TAK-242 and Its Therapeutic Effect on Mouse Sepsis Model. *Br. J. Pharmacol.* **2009**, *157* (7), 1250−1262.
(57) Lenert, P.; Stunz, L.; Yi, A.-K.; Krieg, A. M.; Ashman, R. F. CpG Stimulation of Primary Mouse B Cells Is Blocked by Inhibitory Oligodeoxyribonucleotides at a Site Proximal to NF-κB Activation. *Antisense Nucleic Acid Drug Dev.* **2001**, *11* (4), 247−256.
(58) Davies, D. H.; Liang, X.; Hernandez, J. E.; Randall, A.; Hirst, S.; Mu, Y.; Romero, K. M.; Nguyen, T. T.; Kalantari-Dehaghi, M.; Crotty, S.; et al. Profiling the Humoral Immune Response to Infection by Using Proteome Microarrays: High-Throughput Vaccine and Diagnostic Antigen Discovery. *Proc. Natl. Acad. Sci. U. S. A.* **2005**, *102* (3), 547−552.
(59) Matheu, M. P.; Sen, D.; Cahalan, M. D.; Parker, I. Generation of Bone Marrow Derived Murine Dendritic Cells for Use in 2-Photon Imaging. *J. Visualized Exp.* **2008**, DOI: 10.3791/773.

DOI: 10.1021/acscentsci.5b00274
ACS Cent. Sci. 2015, 1, 439−448